

# Hyperpolarized xenon nuclear spins detected by optical atomic magnetometry

V. V. Yashchuk,<sup>1,\*</sup> J. Granwehr,<sup>2,†</sup> D. F. Kimball,<sup>1,‡</sup> S. M. Rochester,<sup>1,§</sup>  
A. H. Trabesinger,<sup>3,¶</sup> J. T. Urban,<sup>2,\*\*</sup> D. Budker,<sup>1,4,††</sup> and A. Pines<sup>2,‡‡</sup>

<sup>1</sup>*Department of Physics, University of California at Berkeley, Berkeley, California 94720-7300*

<sup>2</sup>*Materials Sciences Division, Lawrence Berkeley National Laboratory, and Department of Chemistry, University of California at Berkeley, Berkeley, California 94720-1460*

<sup>3</sup>*Laboratory of Physical Chemistry ETH-Hönggerberg, CH-8093 Zurich, Switzerland*

<sup>4</sup>*Nuclear Science Division, Lawrence Berkeley National Laboratory, Berkeley, California 94720*

(Dated: December 2, 2024)

We report the use of an atomic magnetometer based on nonlinear magneto-optical rotation with frequency modulated light (FM NMOR) to detect nuclear magnetization of xenon gas. The magnetization of a spin-exchange-polarized xenon sample (1.7 cm<sup>3</sup> at a pressure of 5 bar, natural isotopic abundance, polarization 1 %), prepared remotely to the detection apparatus, is measured with an atomic sensor (which is insensitive to the leading field of 0.45 G applied to the sample; an independent bias field at the sensor is 140  $\mu$ G). An average magnetic field of  $\sim 10$  nG induced by the xenon sample on the 10-cm diameter atomic sensor is detected with signal-to-noise ratio  $\sim 10$ , limited by residual noise in the magnetic environment. The possibility of using modern atomic magnetometers as detectors of nuclear magnetic resonance and in magnetic resonance imaging is discussed. Atomic magnetometers appear to be ideally suited for emerging low-field and remote-detection magnetic resonance applications.

PACS numbers: 07.55.Ge,82.56.Dj,76.60.Pc

Nuclear magnetic resonance (NMR) is a versatile technique for the study of structure and dynamics on both molecular and macroscopic scales, and on time scales from nanoseconds to hours. Spin-polarized <sup>129</sup>Xe (nuclear spin-1/2, magnetic moment  $\mu \approx -0.78 \mu_N$ , where  $\mu_N$  is the nuclear magneton) is particularly well suited for NMR and magnetic-resonance imaging (MRI) studies for several reasons. It is possible to polarize it using the laser-optical-pumping techniques [1]. In contact with various analytes, it displays a wide range of relative chemical shifts of up to several hundred ppm [2, 3], which makes it an ideal probe of its local chemical environment [4]. Finally, it has a long longitudinal relaxation time of several minutes or longer even at low fields. Xenon can also be used in solution, and is especially soluble in organic solvents.

An important recent development in NMR/MRI is the technique of remote detection [5, 6], in which information about an analyte is transferred onto a mobile spin-polarized substance, and is then read out at a different location. This technique allows the separate optimization of the encoding and the detection environment. As the signal in this case is the overall magnetization of the spin-polarized sample, the task is now to read this information out efficiently and with high sensitivity. Detection using superconducting quantum interference devices (SQUIDs) [7] and atomic magnetometers [8] provide an alternative to the traditional techniques involving induction detection in the presence of a strong magnetic field. In fact, SQUIDs have already proven useful in NMR experiments [2, 9].

Atomic magnetometers (the essential components of which consist only of a diode laser, an atomic vapor cell,

and the necessary optics and electronics) are also attractive for NMR applications as they have the potential to be very cheap and compact and—in contrast to SQUIDs, which require cryogenic temperatures—they operate at room temperature. The first use of an atomic magnetometer for detection of the static magnetic field produced by a sample of gaseous nuclear-polarized atoms was reported nearly 35 years ago in the pioneering work of Cohen-Tannoudji *et al.* [10]. In that work, a 6-cm diam. vapor cell containing 5%-optically-polarized <sup>3</sup>He gas at a pressure of 3 torr was placed next to a cell of similar dimensions containing <sup>87</sup>Rb and serving as a sensor of an optical-pumping magnetometer. The 60 nG field produced by the nuclear spins was detected with sensitivity  $\sim 3 \times 10^{-9}$  G/ $\sqrt{\text{Hz}}$ . A similar setup was also used in Ref. [11].

Modern atomic magnetometers utilizing alkali-metal vapors in anti-relaxation-coated cells can achieve sensitivities to magnetic field better than  $10^{-11}$  G/ $\sqrt{\text{Hz}}$ , see, for example, Ref. [12] and review [8]. Recently, a sensitivity of  $5 \times 10^{-12}$  G/ $\sqrt{\text{Hz}}$  was demonstrated [13] with an atomic sensor of a volume of only 0.3 cm<sup>3</sup> where, instead of anti-relaxation coating, buffer gas was used to reduce relaxation in wall collisions, and operation at a high alkali-atom density ensured the rapid spin-exchange-collision regime [14], where spin-relaxation in collisions between alkali atoms is also reduced. Due to such advances, the use of atomic magnetometers for low-field NMR experiments becomes attractive.

With a view toward future NMR applications, particularly remote detection, we have carried out exploratory measurements of samples of gaseous spin-exchange-polarized xenon with a modified version of the

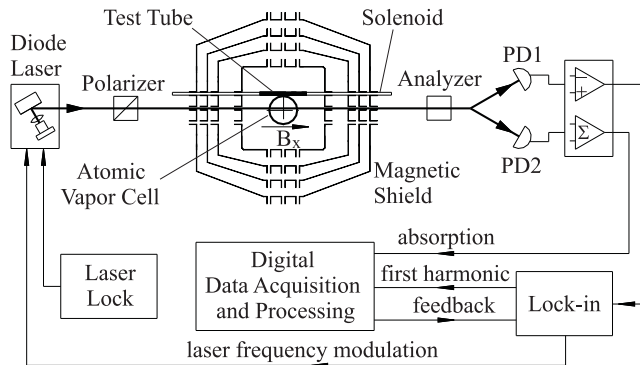


FIG. 1: Atomic magnetometer used for detecting Xe nuclear-spin polarization.

atomic magnetometry apparatus previously described in Refs. [12, 15, 16] (Fig. 1). The apparatus incorporates a 10-cm diameter spherical  $^{87}\text{Rb}$ -vapor cell at room temperature with no buffer gas, whose inner walls are coated [17] with paraffin to reduce spin relaxation in collisions of Rb atoms with the wall. The magnetic-field measurement is based on the technique of nonlinear magneto-optical rotation with frequency-modulated light (FM NMOR) [15]. The key feature of the method is the use of an ultra-narrow resonance arising when the frequency of the light is modulated at twice the Larmor-precession frequency of the Rb atoms (Fig. 2). The magnetometer operates in a closed feedback loop involving digital signal processing, locking to an FM NMOR resonance by adjusting the diode-laser-modulation frequency. The mean frequency of the  $4\ \mu\text{W}$  laser light delivered to the sensor is locked to the D1-resonance using a technique [18] involving an auxiliary Rb-vapor cell (not shown). The atomic sensor cell is placed inside a multi-layer magnetic shield (shielding factor  $\sim 10^6$  [19]) equipped with internal magnetic coils. The FM NMOR magnetometer is intrinsically a scalar device; however, a bias field of  $140\ \mu\text{G}$  applied along the direction of light propagation renders the sensor linearly sensitive only to the average component of the magnetic field produced by the sample in that direction.

The xenon samples of natural isotopic abundance containing about 26% of  $^{129}\text{Xe}$  were prepared using a commercial spin-exchange polarizer (MITI IGI 9800 Xe). A gas mixture of 1% Xe, 10%  $\text{N}_2$ , and 89% He was used. After polarization, xenon was removed from the gas mixture by freezing in a cold finger that was immersed into liquid nitrogen. At the end of the polarization process, the Xe batch was thawed into a sapphire sample tube equipped with a miniature titanium spring-loaded valve mechanism with overall outer diameter of 6.4 mm and sample volume dimensions of 4.8 mm inner diameter and 140 mm length [20]. These materials were chosen to ensure a long

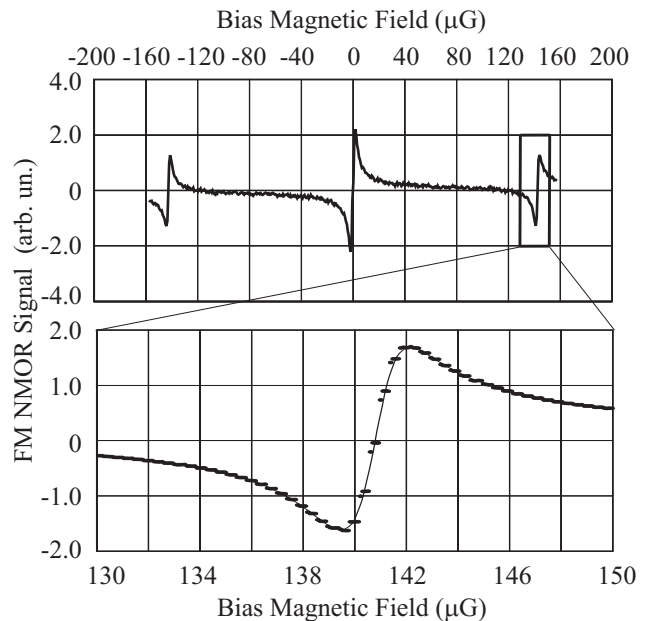


FIG. 2: The FM NMOR resonances recorded with laser-modulation frequency set at 200 Hz. During the operation of the magnetometer, the bias field is fixed and the modulation frequency is locked to the center of a resonance.

spin-polarization relaxation time [21]. The outer diameter of the tube was dictated by the tight constraints given by the geometry of the atomic magnetometer's magnetic shield [19]. The tube was designed for operation with gas pressures of up to 30 bar. The xenon polarization was measured by the polarizer's onboard NMR spectrometer and calibrated using thermally-polarized xenon dissolved in pentane on a Varian Unity Inova NMR spectrometer equipped with an Oxford 7-T magnet. The longitudinal relaxation time constant  $T_1$  in the tube was found to be  $T_1 \approx 45$  min within the 7-T magnet, and typically  $\gtrsim 15$  min in the earth and laboratory fields. For the experimental runs described here, we used samples with total xenon pressure of  $\sim 5$  bar with 4 – 8% initial  $^{129}\text{Xe}$  polarization.

A piercing solenoid (see Fig. 1) was used to apply a leading field of 0.45 G to the xenon sample. The setup is designed so that the leakage field outside of the solenoid has negligible effect on the atomic sensor; field due to the piercing solenoid is a factor of  $\approx 2 \times 10^5$  smaller at the vapor cell, as determined by an auxiliary measurement with the atomic magnetometer (Fig. 3). During the xenon measurement, this leakage field provides a constant magnetic field offset that is much smaller than and transverse to the  $140\ \mu\text{G}$  bias field applied to the atomic sensor. Thus, the FM NMOR measurement is largely insensitive to it.

After introducing spin-exchange-polarized xenon into the tube, the sample is hand-delivered to the atomic

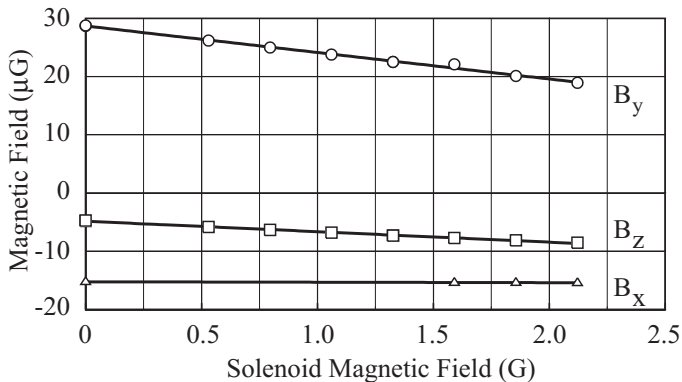


FIG. 3: Auxiliary measurements of the field leaking from the leading-field solenoid. These measurements were performed at the zero-field FM NMOR resonance (Fig. 2), that is sensitive to transverse components of the field. During xenon measurements, the residual fields were nulled with the internal coils.

magnetometry laboratory located in a different building and loaded into the magnetometer apparatus inside the piercing solenoid (Fig. 1). Typically, it takes about 5 min between the completion of xenon gas preparation and the beginning of the atomic magnetometer measurements. Differential measurement is achieved by moving the sample within the piercing solenoid in and out of the position next to the Rb cell where maximal sensitivity to the xenon magnetic field is obtained. This modulation is effective in discriminating between the xenon magnetization signal and the slow drift (typically,  $\sim 1$  nG/min) of the magnetic field within the shield. When the sample tube is in the position where the atomic sensor is most sensitive to its field, the average magnetic field from the xenon magnetization over the volume of the magnetometer sensor cell (equal to the field in the center of the cell) is a factor of 5000 smaller than the field in the sample tube. This suppression factor was calculated from the experimental geometry and verified experimentally by replacing the sample cell with a calibrated solenoid of the same dimensions, and could be greatly reduced with a sensor geometry designed specifically for this application. When the sample tube is moved away to the “out” position, the suppression factor is about two orders of magnitude larger. An example of experimental data is shown in Fig. 4.

With a measurement time of about 3 s per point, we detect the decay of xenon magnetization corresponding to an initial average field at the atomic sensor of about 10 nG with a signal-to-noise ratio (S/N) of about 10, clearly demonstrating the ability of the atomic sensor to detect dc magnetization of a small gaseous sample. It should be emphasized that the S/N obtained in this work is many orders of magnitude lower than what one could obtain with straightforward modifications of this tech-

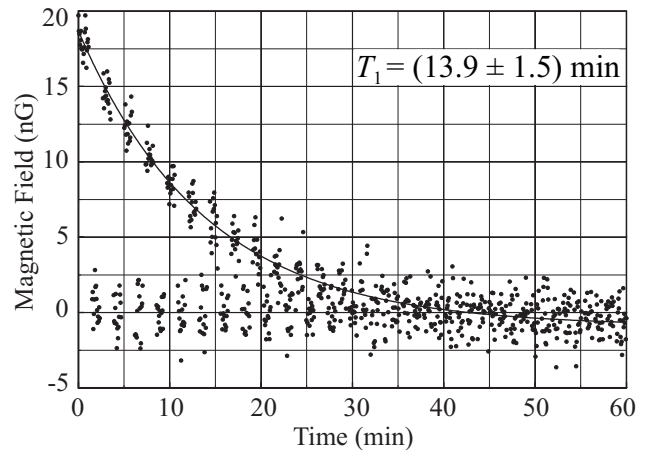


FIG. 4: An example of the Xe-magnetization signal recorded with the atomic magnetometer. Approximately every minute, the xenon sample is moved within the solenoid between the position of maximum and near-zero sensitivity (when the sample is partially outside of the innermost magnetic shield) of the atomic magnetometer to the magnetic field produced by the sample. We have subtracted from the data the overall slow drift due to the temperature drift-related change of the residual magnetization of the shield. This drift is determined from the portion of the data taken when the xenon sample is in the position where the sensor does not feel its magnetization. There is a slight offset of the data ( $\lesssim 1$  nG) due to the diamagnetic susceptibility of the sample tube.

nique. Perhaps most significant would be the improvement of the geometrical suppression factor from 5000 to about 10 with optimized geometry. In addition, the magnetic noise in this experiment is dominated by the fluctuations of the magnetic field within the magnetic shield and exceeds the projected intrinsic sensor noise of our apparatus [12, 15] of  $\lesssim 10^{-11}$  G/ $\sqrt{\text{Hz}}$  by about two orders of magnitude. This noise can be effectively suppressed (as was done, for example, in Ref. [13]) by employing a gradiometric arrangement of magnetic sensors.

With a system consisting of two compact, high-precision atomic magnetometers operating in gradiometric mode, it is possible to measure the magnetization of about  $10^{13}$  fully polarized nuclear (e.g.,  $^{129}\text{Xe}$ ) spins in less than a second with a signal-to-noise of 10. The open geometry of an atomic magnetometer equipped with a piercing solenoid would allow measurements in which polarized samples can be continuously transported through the magnetometer, an important feature for remote detection experiments [5]. Commercial xenon hyperpolarization systems are capable of producing over a liter of xenon gas at 1 bar with typical polarization of  $\sim 8\%$ . Using such a system and an optimized atomic magnetometer, it will be possible to make point-by-point low-field measurements, in which a single-point sample will constitute  $\sim 0.1$  mL of xenon gas whose magnetization will be determined with  $S/N \sim 10^4$  in  $\sim 0.3$  s, allowing

ten thousand single-point measurements to be taken in less than an hour. Faster and/or higher resolution scans can, in principle, be obtained by using multiple atomic sensors in parallel, and/or by reducing the S/N.

In principle, it is also possible to perform manipulations on the nuclear spins within the magnetometer, including adiabatic spin-flips, spin-echoes, etc. This capability may be of interest for ultra-low field NMR studies (leading fields can be as low as  $10^{-7}$  G limited by the magnetic-shielding system; if necessary, much larger leading fields than those used in this work may be applied as well). Ultra-low field NMR with SQUID detection has been recently demonstrated as a powerful tool for analytical chemistry [9]. A useful feature of the present approach is the ability, due to the presence of the piercing solenoid, to apply a leading field to the sample under investigation and an independent bias field to the atomic-magnetometer sensor cell.

In conclusion, we have demonstrated reliable detection of nuclear spin polarization of gaseous samples of spin-exchange-polarized xenon using an atomic magnetometer based on nonlinear magneto-optical rotation with frequency-modulated light. The present apparatus is not optimized for NMR/MRI work, and there is a large ( $\sim 5000$ ) geometrical suppression factor that will be reduced in a future dedicated setup. That setup will also employ a gradiometric arrangement of atomic sensors, thus reducing the presently dominant source of noise resulting from fluctuations and drift of the magnetic field within the magnetic shield. Estimates of the sensitivity of such a device show its great promise as a detector for NMR and MRI studies.

The authors are grateful to Dr. Song-I Han for useful discussions and to A. Vaynberg, T. Millet, and M. Solarz for making crucial parts of the apparatus and technical assistance. This work was supported by the Office of Naval Research (grant N00014-97-1-0214), by NSF, and by the Director, Office of Science, Office of Basic Energy Sciences, Materials Sciences and Nuclear Science Divisions, of the U.S. Department of Energy under contract DE-AC03-76SF00098. J.G. gratefully acknowledges the Swiss National Science Foundation for support through a postdoctoral fellowship.

---

\* Electronic address: yashchuk@socrates.berkeley.edu

† Electronic address: joga@waugh.cchem.berkeley.edu

‡ Electronic address: dfk@uclink4.berkeley.edu

§ Electronic address: simonkeys@yahoo.com

- ¶ Electronic address: Andreas.Trabesinger@nmr.phys.chem.ethz.ch
- \*\* Electronic address: jurban@OCF.Berkeley.EDU
- †† Electronic address: budker@socrates.berkeley.edu
- ‡‡ Electronic address: pines@berkeley.edu
- [1] T. G. Walker and W. Happer, *Rev. Mod. Phys.* **69**, 629 (1997).
  - [2] A. Wong-Foy, S. Saxena, A. J. Moule, H. M. L. Bitter, J. A. Seeley, R. McDermott, J. Clarke, and A. Pines, *J. Mag. Reson.* **157**, 235 (2002).
  - [3] B. M. Goodson, *J. Mag. Reson.* **155**, 157 (2002).
  - [4] M. M. Spence, S. M. Rubin, I. E. Dimitrov, E. J. Ruiz, D. E. Wemmer, A. Pines, S. Q. Yao, F. Tian, and P. G. Schultz, *Proc. Natl. Acad. Sci. U. S. A* **98**, 10654 (2001).
  - [5] A. J. Moule, M. M. Spence, S. I. Han, J. A. Seeley, K. L. Pierce, S. Saxena, and A. Pines, *Proc. Natl. Acad. Sci. U. S. A* **100**, 9122 (2003).
  - [6] J. A. Seeley, S. I. Han, and A. Pines, *J. Mag. Reson.* **167**, 282 (2004).
  - [7] J. Clarke, in *SQUID Sensors: Fundamentals, Fabrication, and Applications*, edited by H. Weinstock (Kluwer Academic, The Netherlands, 1996), pp. 1–62.
  - [8] D. Budker, W. Gawlik, D. F. Kimball, S. M. Rochester, V. V. Yashchuk, and A. Weis, *Rev. Mod. Phys.* **74**, 1153 (2002).
  - [9] R. McDermott, A. H. Trabesinger, M. Muck, E. L. Hahn, A. Pines, and J. Clarke, *Science* **295**, 2247 (2002).
  - [10] C. Cohen-Tannoudji, J. DuPont-Roc, S. Haroche, and F. Laloë, *Phys. Rev. Lett.* **22**, 758 (1969).
  - [11] N. R. Newbury, A. S. Barton, P. Bogorad, G. D. Cates, M. Gatzke, H. Mabuchi, and B. Saam, *Phys. Rev. A* **48**, 558 (1993).
  - [12] D. Budker, D. F. Kimball, S. M. Rochester, V. V. Yashchuk, and M. Zolotarev, *Phys. Rev. A* **62**, 043403 (2000).
  - [13] I. K. Kominis, T. W. Kornack, J. C. Allred, and M. V. Romalis, *Nature* **422**, 596 (2003).
  - [14] W. Happer and A. C. Tam, *Phys. Rev. A* **16**, 1877 (1977).
  - [15] D. Budker, D. F. Kimball, V. V. Yashchuk, and M. Zolotarev, *Phys. Rev. A* **65**, 055403 (2002).
  - [16] Y. P. Malakyan, S. M. Rochester, D. Budker, D. F. Kimball, and V. V. Yashchuk, *Phys. Rev. A* **6901**, 3817 (2004).
  - [17] E. B. Alexandrov, M. V. Balabas, D. Budker, D. English, D. F. Kimball, C. H. Li, and V. V. Yashchuk, *Phys. Rev. A* **66**, 042903/1 (2002).
  - [18] V. V. Yashchuk and D. Budker, *To be published* (2004).
  - [19] V. Yashchuk, D. Budker, and M. Zolotarev, in *Trapped Charged Particles and Fundamental Physics* (Asilomar, CA, USA, 1999), vol. 457 of *AIP Conf. Proc.*, pp. 177–81.
  - [20] V. V. Yashchuk, J. Granwehr, A. Trabesinger, and D. Budker, *To be published* (2004).
  - [21] M. Haake, B. M. Goodson, D. D. Laws, E. Brunner, M. C. Cyrier, R. H. Havlin, and A. Pines, *Chem. Phys. Lett.* **292**, 686 (1998).